

Aligning Forest and Trees in Images and Long Captions for Visually Grounded Understanding

Byeongju Woo¹ Zilin Wang² Byeonghyun Pak¹ Sangwoo Mo³ Stella X. Yu²

Abstract

Large vision-language models such as CLIP struggle with long captions because they align images and texts as undifferentiated wholes. Fine-grained vision-language understanding requires hierarchical semantics capturing both global context and localized details across visual and textual domains. Yet linguistic hierarchies from syntax or semantics rarely match visual organization, and purely visual hierarchies tend to fragment scenes into appearance-driven parts without semantic focus.

We propose CAFT (*Cross-domain Alignment of Forests and Trees*), a hierarchical image-text representation learning framework that aligns global and local semantics across images and long captions without pixel-level supervision. Coupling a fine-to-coarse visual encoder with a hierarchical text transformer, it uses a hierarchical alignment loss that matches whole images with whole captions while biasing region-sentence correspondences, so that coarse semantics are built from fine-grained evidence rather than from aggregation untethered to part-level grounding.

Trained on 30M image-text pairs, CAFT achieves state-of-the-art performance on six long-text retrieval benchmarks and exhibits strong scaling behavior. Experiments show that hierarchical cross-domain alignment enables fine-grained, visually grounded image-text representations to emerge without explicit region-level supervision.

1. Introduction

A *red bus* is never just a *red bus* (Figure 1): *a modern red double-decker, labeled route 38, pedestrians nearby, a hatchback car passing, a stone building with arched windows and a flagpole on its roof*. Such long text can be both

¹Agency for Defence Development (ADD), Korea ²University of Michigan ³POSTECH. Correspondence to: Byeongju Woo <byeongju@umich.edu>.

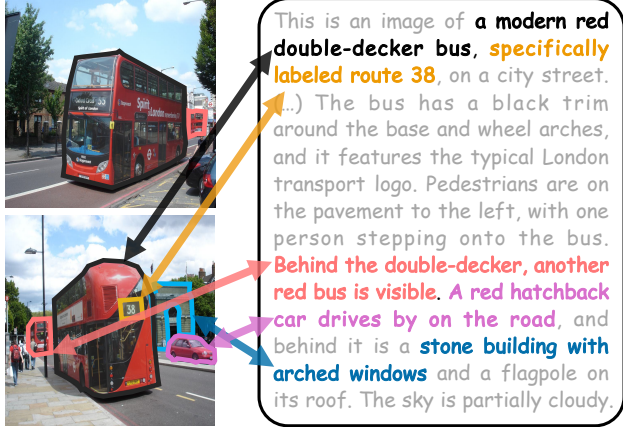


Figure 1. Long-text image retrieval demands grounded understanding. Identifying the correct image (bottom) requires recognizing both its coarse composition (*what major elements are present: bus, car, building etc.*) and its fine-grained details (*what each element is: a modern red double-decker bus labeled route 38*). In the wrong image (top), a long caption causes the baseline model to latch onto some dominant descriptions while neglecting others, leading to errors in both scene composition and local details. This example illustrates the need for models that align visual and textual structure across scales, seeing both the *forest* and the *trees*.

a blessing and a trap: Every extra clause adds detail but also distraction. A model that merely matches whole captions to whole images may seize on a dominant yet incomplete cue (Radford et al., 2021; Zhang et al., 2024; Wu et al., 2024), overlooking critical details such as the *bus number* or the broader scene composition involving *buses*, a *car*, and a *stone building*. To get it right, a system must see both *forest* and *trees*, within and across visual and textual domains (Biederman, 1987; Maurer et al., 2002).

Visual understanding requires organizing *image patches* into *objects*, and *objects* into a coherent *scene*, while capturing spatial and compositional relationships such as a *person stepping onto a bus*, a *car passing by*, or a *building behind the vehicles* (Fukushima, 1980; Kuzovkin et al., 2018). Language can assist this process, but not through its standard *syntactic* or *semantic* representations alone (Figure 2). *Parse trees* encode grammatical structure (Shi et al., 2019; Drozdov et al., 2019), while *semantic graphs* emphasize events and abstract relations rather than the geometric and

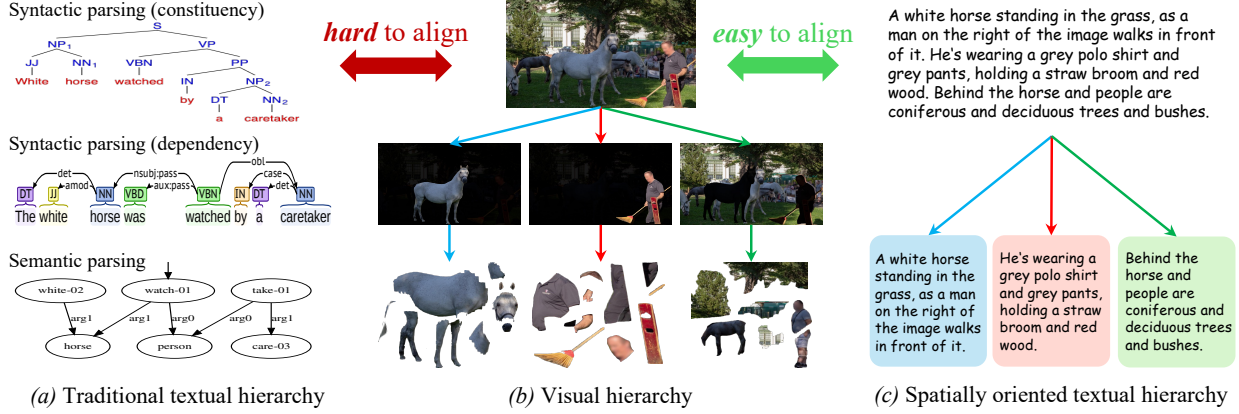


Figure 2. **Vision-language understanding requires hierarchical semantics to be aligned across domains.** Traditional textual hierarchies, such as syntactic parse trees or semantic graphs, do not naturally correspond to the spatial organization of visual scenes. In contrast, spatially oriented textual hierarchies, where each part describes a distinct image region, align naturally with visual hierarchies.

compositional organization of *buses*, *cars*, and *buildings* (Johnson et al., 2015; Zellers et al., 2018; Yang et al., 2018).

What is needed instead is a hierarchical textual representation that mirrors how scenes are composed, enabling textual units at multiple levels of granularity to be grounded in corresponding visual components and their relationships.

We propose CAFT that operationalizes long-text grounded understanding by *Cross-domain Alignment of Forests and Trees*, based on three design insights.

1. Spatially structured long captions. Many long captions decompose into sentences describing scene components. We leverage this structure to induce a *textual hierarchy*, in which each sentence represents a candidate semantic unit that may be grounded in a corresponding visual component, although the specific region it corresponds to is unknown and must be discovered.

2. Coherent within-domain hierarchies. Both images and texts are represented hierarchically, with coarse semantics explicitly constructed from finer-grained evidence rather than bypassing it. On the text side, we design a *hierarchical text transformer* that first encodes sentence-level units in parallel and then composes them into a global description. On the visual side, we employ a fine-to-coarse visual encoder that preserves part-whole structure, ensuring that a *red double-decker bus labeled route 38* is not indiscriminately aggregated into a generic *bus*. These design choices ensure that global semantics are composed from fine-grained, grounded evidence, rather than being learned by indiscriminately aggregating details into a single global representation.

3. Hierarchical cross-domain alignment. At the core of CAFT is a hierarchical alignment objective that jointly discovers aligned *parts* and *wholes* across image and text, with visual regions discovered without any image-

domain supervision and aligned to sentence-level units without explicit image–text cross-domain correspondences. The objective matches whole images with whole captions while biasing mid-level correspondences between visual components and sentence-level textual units, so that global scene semantics are grounded in localized evidence rather than dominated by a single salient cue.

Trained on 30M image–text pairs, CAFT exhibits strong scaling behavior and achieves state-of-the-art performance across six long-text retrieval benchmarks. Beyond aggregate metrics, CAFT demonstrates qualitatively stronger grounded understanding. As shown in Figure 3, it clearly distinguishes between visually similar scenes by attending to fine-grained caption components and grounding them in the appropriate image regions, whereas baseline models waver among look-alikes.

These gains stem from attending to both *trees* and *forest* simultaneously. Rather than collapsing a long caption or an image through indiscriminate aggregation, CAFT preserves and aligns fine-grained components, grounding each caption segment in corresponding visual evidence. By explicitly accounting for individual details, the model constructs more accurate global scene representations, enabling reliable discrimination between subtly different scenes. This compositional grounding explains why CAFT consistently outperforms a range of alignment baselines, particularly in long-text retrieval settings where attending to only the forest or only the trees – without modeling their hierarchical relationship – leads to ambiguous matches.

An additional and exciting outcome is that CAFT acquires meaningful segmentation from images and text alone, enabling unsupervised visual parsing without any segmentation annotations. Benchmarked on zero-shot referring segmentation, CAFT significantly outperforms representative methods such as GroupViT (Xu et al., 2022) and MaskCLIP

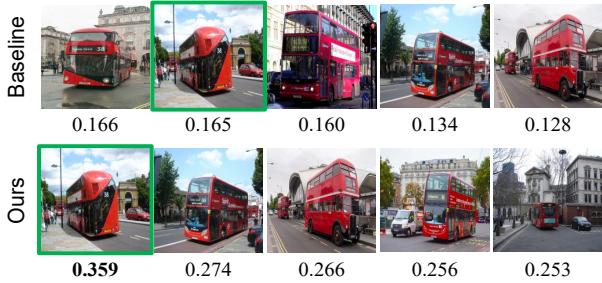
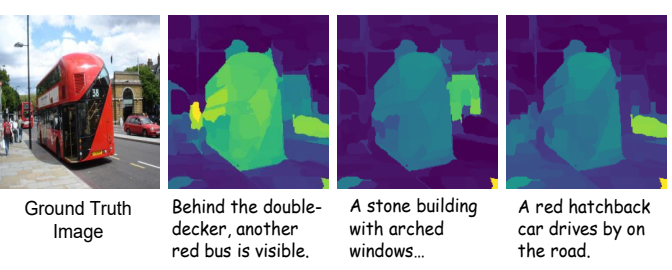
a) Top-5 image retrievals for the example in Figure 1.**b)** Attention maps of individual sub-captions.

Figure 3. CAFT demonstrates fine-grained, grounded vision-language understanding. **a)** Among visually similar bus images, the baseline method, FLAIR, wavers among look-alikes, whereas our proposed CAFT selects the correct match with a clearly higher retrieval score. **b)** This improvement arises from representations that attend individual sub-captions to their corresponding image regions, emerging naturally without explicit supervision.

(Zhou et al., 2022). These results corroborate that aligning natural spatial hierarchies across image and text is key to visually grounded understanding.

2. Related Work

CLIP with long-text capability has recently been studied as a promising direction for handling detailed descriptions. This capability is enabled by synthetic long captions generated by MLLMs (Zheng et al., 2024; Chen et al., 2024), which provide richer supervision than raw web annotations. To adapt longer input, several studies (Zhang et al., 2024; Najdenkoska et al., 2024; Choi et al., 2025; Asokan et al., 2025) extend CLIP’s capacity by enlarging the positional encoding from 77 to 248 tokens, while LoTLIP (Wu et al., 2024) explores this from scratch. However, these methods struggle to capture both the local details in sub-captions and the holistic semantics of the full caption. To address this limitation, we propose a hierarchical text transformer that effectively captures both local and holistic semantics.

Visually grounded understanding has been extensively explored for fine-grained vision-language tasks (Antol et al., 2015; Vinyals et al., 2015; Pak et al., 2024; Wang et al., 2025). Such approaches typically ground local elements, such as noun phrases, with dense annotations (e.g., bounding boxes). For example, GLIP (Li et al., 2022) aligns phrases with regions using large-scale human-labeled data, while GOAL (Choi et al., 2025) employs SAM to obtain regions of interest (Kirillov et al., 2023) and aligns them with sub-captions through a pretrained CLIP. More recently, FLAIR(Xiao et al., 2025) introduces text-conditioned attention pooling to localize sentences on visual patches, enabling fine-grained representations without dense labels. Building on FLAIR’s attention pooling, CAFT learns implicit grounding but integrates fine-grained regions into holistic semantics—capabilities not explored in prior works.

3. Aligning Forest and Trees Cross Domains

We propose **CAFT** (Cross-domain Alignment of Forests and Trees), a hierarchical image-text representation learning framework that aligns global and local semantics across images and long captions. In this section, we first detail how we construct the visual hierarchy (Section 3.1) and the textual hierarchy tailored for long captions (Section 3.2), then describe the hierarchical alignment of the visual and textual domains (Section 3.3).

3.1. Part-Whole Structure in Vision

To understand complex visual scenes, people parse them into part-whole hierarchies (Hinton, 1979), providing *what-is-where* substantiation and compositional structure. Our objective in the vision branch is to learn such an explicit part-whole hierarchy for recognition and by recognition.

To this end, we construct a *fine-to-coarse visual encoder* that progressively clusters fine-grained tokens into coarser segment tokens based on semantic similarity as in the graph pooling of CAST (Ke et al., 2023). This hierarchical segmentation correlates with the part-whole relationship, which we uncover solely through language supervision.

Specifically, our model starts from 196 superpixel tokens and groups them into 64, 32, and 16 segment tokens. Among these, the segment tokens in the second stage, denoted as $\mathbf{v}^{\text{fine}} \in \mathbb{R}^{64 \times C}$, are used for the part-level alignment, while the [CLS] token from the final layer, denoted as $\mathbf{v}^{\text{coarse}} \in \mathbb{R}^C$, serves as the representation for the whole-level alignment. This selection ensures that lower levels capture localized and finer-grained object details, while higher levels encode holistic scene semantics. Consequently, finer segment features are effective for object-level details, whereas coarser segment features better capture scene-level semantics. This hierarchical design provides a natural basis for aligning visual representations at different granularities with textual descriptions of varying scope.

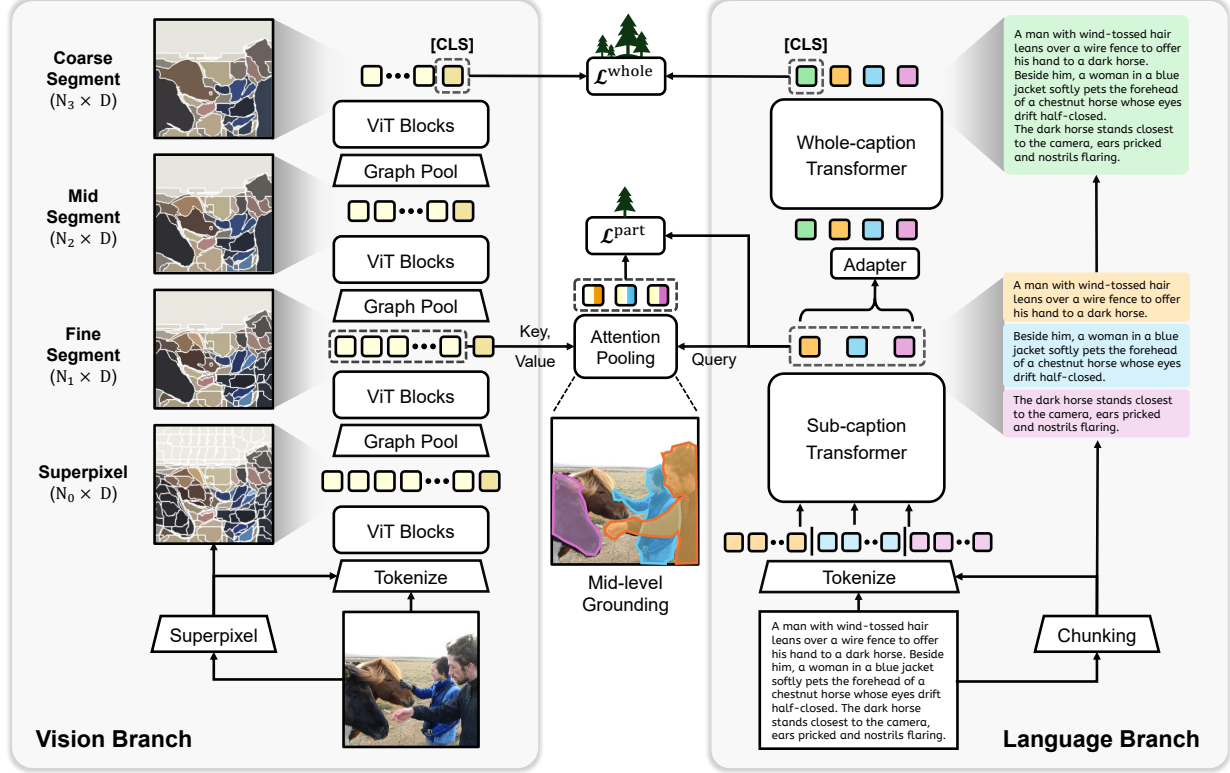


Figure 4. Overview of CAFT. The model constructs hierarchical representations for both vision and language, aligning them at matched granularities. **Vision Branch:** Starting from superpixel tokens, the model performs fine-to-coarse scene parsing via progressive token grouping interleaved with ViT blocks. **Language Branch:** A Sub-caption Transformer encodes each text chunk independently, followed by a Whole-caption Transformer that aggregates them into a holistic embedding. **Alignment:** We establish a bottom-up hierarchy where mid-level visual features align with sub-caption embeddings for localized grounding (*aligning trees*), while top-level visual features align with whole-caption embeddings to capture global scene semantics (*aligning forest*).

3.2. Part-Whole Structure in Language

Aligning the visual hierarchy with the textual hierarchy in a one-to-one manner is highly challenging. Whether the textual hierarchy is semantic or syntactic, elements that are close in visual appearance may be far apart in textual meaning, and vice versa. However, from long captions we identify a new *spatial hierarchy* that aligns well with the visual hierarchy. Previous work (Zheng et al., 2024) observed that each sub-caption of a long caption tends to describe a specific part of the scene (e.g., an object, a part of an object, or background context). We therefore interpret the hierarchy between sub-captions and the whole long caption as corresponding to the part-whole structure of the image. To effectively capture the hierarchical structure where sub-captions compose a long caption, we propose a *hierarchical text transformer*, with a divide-and-conquer manner: (1) Sub-caption Transformer firstly encodes each sub-caption *independently* to learn a distinct representation, and (2) Whole-caption Transformer encodes the whole long caption from these sub-caption embeddings.

Chunking. We first obtain sub-captions by splitting the long caption into N chunks T_1, T_2, \dots, T_N : we split the

original caption into individual sentences following DreamLIP (Zheng et al., 2024), and then concatenate 1-3 consecutive sentences into each chunk. See more details in the Appendix B.2.

Sub-caption Transformer. Next, we independently forward each chunk through Sub-caption Transformer to encode N sub-caption embeddings \mathbf{t}^{sub} .

$$\mathbf{t}_k^{\text{sub}} = \text{Transformer}_{\text{sub}}(\text{Tokenize}(T_k)) \in \mathbb{R}^D, \quad (1)$$

$$\mathbf{t}^{\text{sub}} = \{\mathbf{t}_k^{\text{sub}}\}_{k=1}^N \in \mathbb{R}^{N \times D}. \quad (2)$$

Whole-caption Transformer. Finally, we obtain the whole caption embedding $\mathbf{t}^{\text{whole}} \in \mathbb{R}^D$ by feeding the sub-caption embeddings together with a [CLS] token into the Whole-caption Transformer. Before feeding, we refine \mathbf{t}^{sub} using a light-weight residual MLP adapter (Gao et al., 2024), yielding the adapted representations $\tilde{\mathbf{t}}^{\text{sub}}$:

$$\mathbf{t}^{\text{whole}} = \text{Transformer}_{\text{whole}}(\tilde{\mathbf{t}}^{\text{sub}}; [\text{CLS}]) \in \mathbb{R}^D \quad (3)$$

3.3. Hierarchical Vision-Language Alignment

Training Batch Construction. We train CAFT from scratch on a synthetic long text-image paired dataset, where each

image is annotated with multiple long and short captions. At each iteration, we construct a batch of B images, each image I_i paired with K positive sub-captions $\{T_{i_k}\}_{k=1}^K$. Among the K sub-captions, the first N sub-captions are derived from a single long caption, while the remaining $(K-N)$ sub-captions are sampled from multiple captions. Therefore, the Whole-caption Transformer takes only the first N sub-captions for its input. The resulting batch input and hierarchical outputs are therefore constructed as follows:

$$\text{batched_input} : \{(I_i, \{T_{i_k}\}_{k=1}^K)\}_{i=1}^B, \quad (4)$$

$$\text{intermediate_outputs} : \{(\mathbf{v}_i^{\text{fine}}, \{\mathbf{t}_{i_k}^{\text{sub}}\}_{k=1}^K)\}_{i=1}^B, \quad (5)$$

$$\text{final_outputs} : \{(\mathbf{v}_i^{\text{coarse}}, \mathbf{t}_i^{\text{whole}})\}_{i=1}^B \quad (6)$$

Part-level Text-grounded Sigmoid Loss aim to align each sub-caption feature with its corresponding visual region features without dense annotation (e.g., bounding box). Following FLAIR, we adopt an attention pooling module (Ilse et al., 2018) to obtain text-grounded visual features. Let $\mathbf{v}_i^{\text{fine}}$ denote visual segment features from image i , and $\mathbf{t}_{j_k}^{\text{sub}}$ denote k -th sub-caption features from caption j . Then attention pooling computes a text-grounded visual feature:

$$\mathbf{v}_{i,j_k}^{\text{tg}} = \text{AttnPool}(\mathbf{t}_{j_k}^{\text{sub}}, \mathbf{v}_i^{\text{fine}}, \mathbf{v}_i^{\text{fine}}) \in \mathbb{R}^D \quad (7)$$

This operation aggregates the visual segments relevant to the given sub-caption query $\mathbf{t}_{j_k}^{\text{sub}}$ via attention scores. We then compare $\mathbf{v}_{i,j_k}^{\text{tg}}$ again with the query $\mathbf{t}_{j_k}^{\text{sub}}$:

$$\mathcal{L}_{i,j,k}^{\text{part}} = -\log \sigma(\tau_p \langle \mathbf{v}_{i,j_k}^{\text{tg}}, \mathbf{t}_{j_k}^{\text{sub}} \rangle + b_p). \quad (8)$$

where τ_{part} and b_{part} are a learnable temperature and a bias, respectively, $\langle \cdot, \cdot \rangle$ denotes cosine similarity, and $\sigma(\cdot)$ is the sigmoid function. The label $y_{i,j}$ indicates whether the pair is positive or negative: $y_{i,j}=+1$ for a positive pair $(\mathbf{v}_{i,i_k}^{\text{tg}}, \mathbf{t}_{i_k}^{\text{sub}})$, and $y_{i,j}=-1$ for a negative pair (when $i \neq j$).

Whole-level Sigmoid Loss aims to align the global image feature $\mathbf{v}_i^{\text{coarse}}$ with the whole caption feature $\mathbf{t}_i^{\text{whole}}$, in contrast to FLAIR, which aligns the global image feature with multiple sub-captions.

$$\mathcal{L}_{i,j}^{\text{whole}} = -\log \sigma(\tau_w \langle \mathbf{v}_i^{\text{coarse}}, \mathbf{t}_j^{\text{whole}} \rangle + b_w). \quad (9)$$

We use separate learnable parameters for the whole-level sigmoid loss: τ_w and b_w , distinct from the part-level ones. We use the same $y_{i,j}$ as in part-level one.

Optimization. We optimize CAFT with two proposed loss functions: $\mathcal{L} = \mathcal{L}^{\text{part}} + \mathcal{L}^{\text{whole}}$. The $\mathcal{L}^{\text{part}}$ encourages alignment between the visual region and sub-captions at the intermediate layer, while the $\mathcal{L}^{\text{whole}}$ enforces alignment between the entire image and long caption at the final layer. We adopt a sigmoid loss instead of softmax for both $\mathcal{L}^{\text{part}}$ and $\mathcal{L}^{\text{whole}}$. Sigmoid is not only more stable when the batch size is small

but also effective at dealing with multiple positives (Zhai et al., 2023).

Inference. Following standard practice (Radford et al., 2021), CAFT computes the image-text alignment score using the whole-level similarity $\langle \mathbf{v}_i^{\text{coarse}}, \mathbf{t}_j^{\text{whole}} \rangle$.

CAFT++. We further introduce CAFT++, which shares the same trained model as CAFT, but differs only in inference mode. In CAFT++, the alignment score is computed as a weighted sum of whole-level and part-level similarities. The effect of the weighting scheme is analyzed in Table 4.

$$s_{ij} = (1 - \alpha) \cdot \langle \mathbf{v}_i^{\text{coarse}}, \mathbf{t}_j^{\text{whole}} \rangle + \alpha \cdot \sum_k \langle \mathbf{v}_{i,j}^{\text{tg}}, \mathbf{t}_{j_k}^{\text{sub}} \rangle \quad (10)$$

4. Experiments

To assess the fine-grained vision-language understanding of CAFT, we first evaluate image-text retrieval on long-caption benchmarks (Section 4.2). We also investigate CAFT’s visual grounding capability to provide insights into how fine-grained understanding is facilitated by grounded recognition (Section 4.3). Finally, we conduct ablation studies to analyze the contributions of each component within our hierarchical learning framework (Section 4.4).

4.1. Setup

Training Datasets. We train CAFT on the re-captioned datasets from DreamLIP (Zheng et al., 2024), which provide long, detailed captions. This dataset consists of CC3M-recap, CC12M-recap, and YFCC15M-recap, which are aggregated into a unified 30M-sample corpus (Merged-30M).

Implementation Details. Our vision encoder is comparable in size to ViT-B/16 (Dosovitskiy et al., 2020), with an input resolution of 224×224 . We follow the vanilla Transformer architecture (Vaswani et al., 2017) for the text encoder, except for adopting a two-stage design: the Sub-caption Transformer ($L_1 = 8$) and a Whole-caption Transformer ($L_2 = 4$). The total depth ($L = 12$) aligns with the original CLIP text encoder (Radford et al., 2021). While the sub-caption context length is set to 77, the whole-caption uses a context length of $N = 4$, the chunk size. Both image and text features use a 512-dimensional embedding. For a fair comparison with FLAIR, we adopt their training hyperparameters but reduce the batch size to 2K due to GPU memory constraints. We maintain $K = 8$ sub-captions per image. Following SigLIP (Zhai et al., 2023), the learnable temperature parameters (τ_p, τ_w) and bias terms (b_p, b_w) are initialized to 0.07 and -10, respectively. Training was conducted on 8 A100 (80GB) GPUs, and training on Merged-30M required approximately 5 days. Further details are provided in Appendix A.1.

Table 1. CAFT achieves state-of-the-art results on zero-shot long text-image retrieval tasks. I2T and T2I indicate the R@1 score on image-to-text and text-to-image retrieval, respectively. The best results are **bold**, second-best are underlined, and \dagger denotes the previous state-of-the-art results for each benchmark. All models use ViT-B/16 as the vision encoder. DCI and DOCCI use human-annotated captions, while the other datasets rely on VLM-generated synthetic captions and generally achieve higher scores. Both CAFT and CAFT++ consistently outperform prior methods across all benchmarks by large margins.

Method	Data	DCI		DOCCI		SV-1k		SV-10k		Urban-1k		IIW	
		I2T	T2I										
<i>Trained on Short-Captions Only</i>													
OpenCLIP	2B	56.0	55.4	-	-	90.3	87.7	69.6	66.8	69.5	65.8	-	-
LiT	100M	41.7	40.9	-	-	86.0	80.0	61.4	50.6	-	-	-	-
ALIGN	700M	56.5	57.4	-	-	86.3	85.3	65.1	62.7	-	-	-	-
SigLIP	10B	57.7	56.2	-	-	85.8	83.4	83.4	63.0	62.7	62.1	-	-
<i>Trained on Short Captions \rightarrow Finetuned on Long-Captions</i>													
Long-CLIP	400M \rightarrow 1M	47.4	44.1	-	-	90.6	87.4	73.1	62.0	78.9	79.5	-	-
FineLIP	400M \rightarrow 1M	-	-	77.1 \dagger	79.5 \dagger	-	-	-	-	90.7 \dagger	89.3 \dagger	-	-
TULIP	400M \rightarrow 1M	-	-	-	-	98.6 \dagger	98.6 \dagger	-	-	88.1	86.6	-	-
FG-CLIP	400M \rightarrow 1.6B	61.8	60.6	-	-	96.7	94.9	-	-	-	-	-	-
<i>Trained on Long-Captions from Scratch</i>													
LoTLIP	100M	62.1 \dagger	61.0	-	-	95.5	86.8	86.8	81.4	-	-	94.0 \dagger	92.5 \dagger
FLAIR	30M	61.3	66.2 \dagger	70.3	72.6	98.5	98.0	90.3 \dagger	89.4 \dagger	83.6	87.7	91.3	91.5
CAFT (ours)	30M	69.4	69.4	80.6	80.4	99.0	98.8	95.1	94.5	93.6	93.9	97.4	96.1
CAFT++ (ours)	30M	69.7	72.4	80.4	82.0	99.5	99.0	95.5	94.8	93.6	95.4	97.6	97.4
<i>vs. previous SOTA</i>		+7.6	+6.2	+3.3	+2.5	+0.9	+0.4	+5.2	+5.4	+2.9	+6.1	+3.6	+4.9

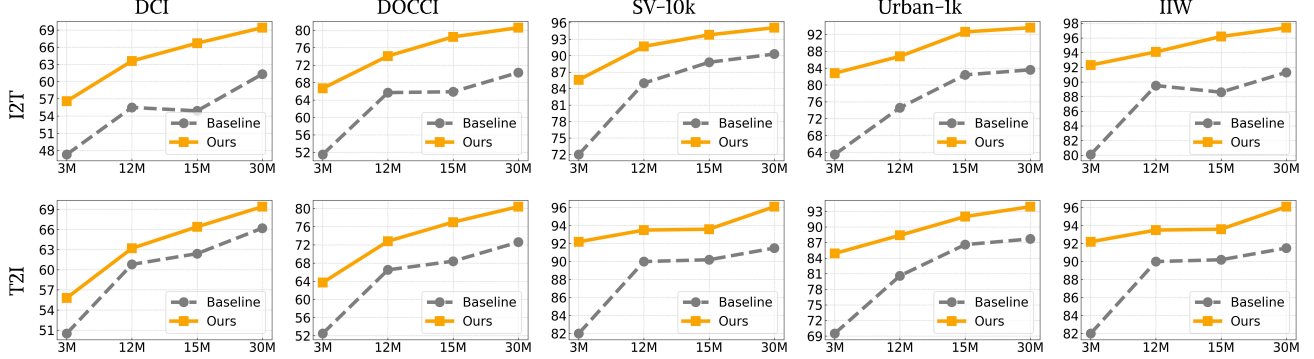


Figure 5. CAFT exhibits strong scaling behavior. We compare CAFT (Ours) with FLAIR (Baseline) across increasing training set sizes (3M, 12M, 15M, and 30M). As the training data scales, our CAFT consistently outperforms the baseline, indicating robust scaling behavior enabled by our hierarchical inductive bias.

4.2. Image-Text Retrieval

Evaluation Benchmark. We evaluate Recall@1 (R@1) for long text-image cross-modal retrieval on six widely used benchmarks: DCI (Urbanek et al., 2024), DOCCI (Onoe et al., 2024), ShareGPT4V-1k (Chen et al., 2024), ShareGPT4V-10k (Chen et al., 2024), Urban-1k (Zhang et al., 2024), and IIW (Garg et al., 2024). Detailed statistics for each dataset are provided in Appendix A.2.

Comparison with State-of-the-art. We categorize prior work into three settings: (i) models trained only on short captions, (ii) models pre-trained on short captions and subsequently fine-tuned on long captions, and (iii) models trained from scratch on long captions. Table 1 provides extensive comparison across six long-caption benchmarks (DCI,

DOCCI, SV-1k, SV-10k, Urban-1k, and IIW), a significantly broader scope than the two or three datasets typically reported in most existing studies. Within this unified setting, CAFT achieves state-of-the-art performance, outperforming FLAIR at the same data scale (30M pairs) and surpassing fine-tuned models despite using far fewer pre-training samples. Furthermore, CAFT++ yields consistent additional gains by incorporating part-level similarity during inference. These results highlight both the effectiveness and data efficiency of our hierarchical design for long-caption retrieval.

Scaling Behavior. Across scales from 3M to 30M pairs, CAFT consistently outperforms FLAIR with a similar scaling slope (Figure 5). These results demonstrate that our hierarchical inductive bias is compatible with scaling laws and provides superior data efficiency compared to FLAIR.

4.3. Visual Grounding

Visual grounding refers to the ability of a model to localize image regions corresponding to a given textual description (Plummer et al., 2015). In this section, we investigate how well CAFT grounds sub-caption descriptions to their corresponding spatial regions, which support fine-grained, grounded recognition.

Qualitative Results. We visualize attention maps from the AttnPool module in Figure 6 to evaluate how CAFT localizes sub-captions. As shown in the first example, CAFT accurately grounds both salient objects (a car) and background elements (the sky). Notably, the fourth row demonstrates the model’s ability to ground entities at multiple levels of granularity, capturing both the entire object (e.g., an elephant) and its fine-grained details (e.g., logos). Furthermore, CAFT exhibits a sophisticated compositional understanding; in the phrase “*Behind the car lies the prominent Big Ben*,” the model attends to both entities but correctly prioritizes the subject (Big Ben) over the spatial reference (car). Further examples are available in Appendix E.

Quantitative Results. We evaluate visual grounding performance across multiple referring image segmentation benchmarks. Given a target image and a referring text description, we leverage the attention maps visualized in Figure 6 and apply Otsu thresholding (Otsu et al., 1975) to obtain binary segmentation masks. Following the evaluation protocol of SaG (Kim et al., 2023), we report mIoU on the RefCOCO, RefCOCO+ (Yu et al., 2016), and GRef (Mao et al., 2016). We compare CAFT with prior approaches trained solely on image-text pairs, including FLAIR which is assessed using the same attention-based segmentation procedure as ours. As shown in Table 2, CAFT consistently outperforms the baseline and demonstrates strong visual grounding compared to previous representative zero-shot methods such as GroupViT (Xu et al., 2022) and MaskCLIP (Zhou et al., 2022). These results indicate that CAFT naturally learns grounded representations that align textual descriptions with spatial regions, without any segmentation supervision. Further analysis on FG-OVD (Bianchi et al., 2024) benchmark is provided in Appendix C.

Emergence of Compositional Understanding. The visual grounding capabilities demonstrated above provide a mechanistic explanation for the improvements in fine-grained tasks (Table 1). Notably, this grounding property emerges at mid-level representations from both the vision and language branches. By constructing holistic representations from these grounded local semantics—rather than processing image and text as undifferentiated wholes—our model successfully captures and leverages rich, fine-grained evidence. This bottom-up integration leads to a robust and compositional understanding essential for fine-grained retrieval.

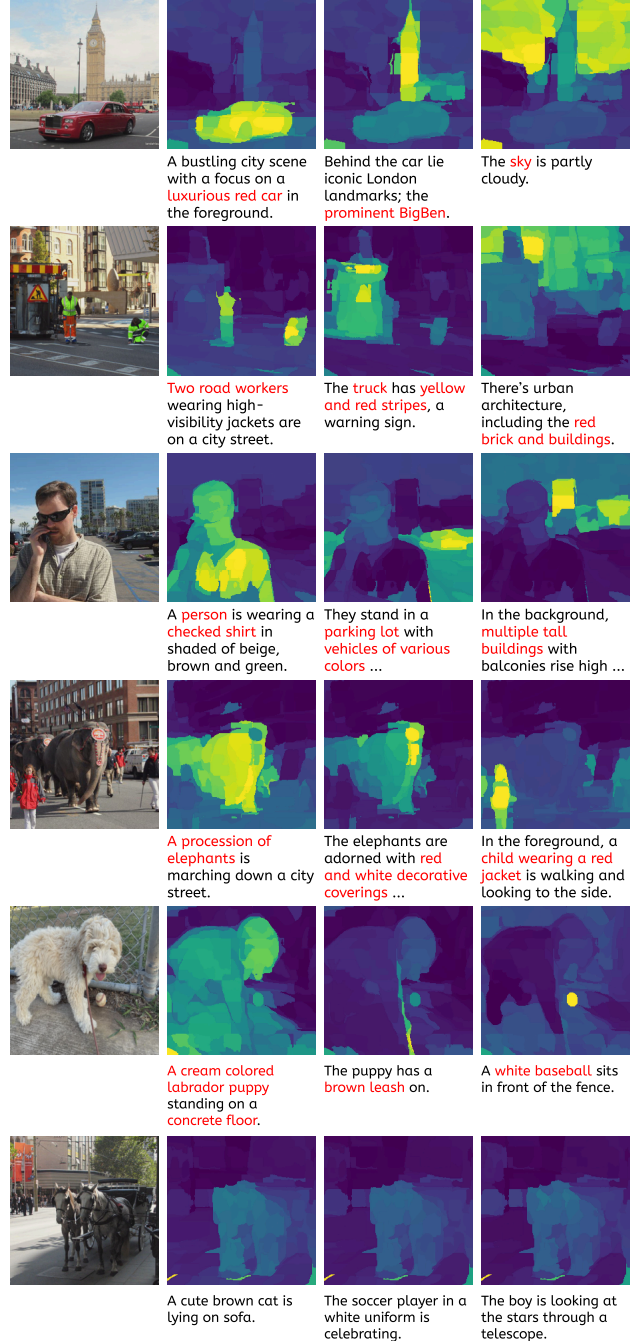


Figure 6. CAFT provides spatially precise grounding. We show head-averaged attention maps from the AttnPool module for each sub-caption. CAFT precisely localizes relevant regions across different scales and positions, with sharp, object-aware boundaries. Notably, the maps exhibit inactivation when provided with irrelevant captions (bottom row), demonstrating robustness to spurious grounding and mismatched semantic cues.

4.4. Ablation Studies

Our ablation study examines the contribution of each component in our hierarchical learning framework: **i) visual hierarchy** based on fine-to-coarse superpixel grouping in-

Table 2. Zero-shot Referring Image Segmentation. We report mIoU for models trained without dense mask supervision. CAFT consistently outperforms both prior methods and the baseline FLAIR across all splits.

Method	RefCOCO			RefCOCO+			Gref val
	val	testA	testB	val	testA	testB	
GViT	7.99	6.16	10.51	8.49	6.79	10.59	10.68
MCLIP	11.52	11.85	12.06	11.87	12.01	12.57	12.74
SaG	21.80	19.00	24.96	22.20	19.86	24.85	25.89
FLAIR	19.79	19.76	19.97	18.49	18.25	18.86	20.21
CAFT	28.85	30.81	28.53	28.46	29.82	28.32	31.39

Table 3. Ablation study from FLAIR to CAFT. Relative to FLAIR, we propose three novel designs: i) **Visual hierarchy**: inducing superpixel tokens and fine-to-coarse token grouping, ii) **Textual hierarchy**: employing hierarchical text transformer, iii) **Hierarchical loss**: adding part-level loss in mid-level representation, and whole-level loss in final-layer representation. All three components contribute to the overall performance gains, together leading to the final CAFT.

Method	DCI		SV-10k		IIW	
	I2T	T2I	I2T	T2I	I2T	T2I
FLAIR	48.3	52.0	73.3	72.1	80.4	83.5
+ Visual hierarchy	49.8	54.1	76.1	74.7	82.5	83.8
+ Textual hierarchy	53.4	50.0	82.3	82.4	91.0	87.3
+ Hierarchical loss	56.6	55.8	85.6	84.7	92.3	92.2
- Part-level alignment	51.4	54.1	82.1	82.2	88.4	86.9

stead of flat ViT, ii) **textual hierarchy** implemented with the hierarchical text transformer that captures both sub-caption and whole-caption embeddings, and iii) **hierarchical alignment loss**, which induces part-level grounding followed by whole-level matching. All experiments are conducted on CC3M-recap with a batch size of 2K, starting from the FLAIR baseline.

Visual Hierarchy. Our ablation study demonstrates that fine-to-coarse grouping is essential for fine-grained vision-language understanding (second row). Unlike a plain ViT that processes images as uniform patches, our CAFT incorporates superpixel tokens and fine-to-coarse grouping modules for structured understanding of complex visual scenes. The inductive bias inherent in visual hierarchies facilitates natural part-level grouping, enabling the encoder to capture both fine details and holistic semantics, which results in consistent performance gains across all datasets.

Textual Hierarchy. In our ablations, the hierarchical text transformer for the text encoder yields the largest single performance gain (third row), suggesting that language modeling plays a more critical role than visual modeling in long-text image pretraining. This improvement stems from how the hierarchical text transformer processes long captions. While CLIP’s text encoder flattens long captions,

Table 4. Ablation study on weighting factor α . We evaluate retrieval performance using an image-text alignment score computed as a weighted sum of whole-level and part-level similarities, defined in Equation (10). The default setting with $\alpha = 0.0$ corresponds to CAFT, while $\alpha = 0.3$, which achieves the best overall performance, is adopted as CAFT++.

α	DCI		SV-10k		Urban-1k		IIW	
	I2T	T2I	I2T	T2I	I2T	T2I	I2T	T2I
0.0 (whole)	69.4	69.4	95.1	94.5	93.6	93.9	97.4	96.1
0.3	69.7	72.4	95.5	94.8	93.6	95.4	97.5	97.4
0.7	63.2	74.1	94.3	94.3	92.2	96.3	97.4	97.9
1.0 (part)	50.5	71.6	90.3	92.3	86.2	94.6	95.3	97.4

conflating local and global semantics, our hierarchical transformer first encodes each sub-caption and then composes them into a whole-caption representation. This design preserves fine-grained local details while supporting holistic semantic understanding. Such hierarchical encoding complements the visual hierarchy and enables long captions to serve as effective supervision for fine-grained grounding. Furthermore, our hierarchical text encoder enables processing of longer inputs without being truncated by the 77-token context limit.

Hierarchical Alignment Loss. Simply adopting hierarchical encoders for both modalities is insufficient without explicit guidance to align part- and whole-level captions with their corresponding visual regions. The results in the fourth row demonstrate that our hierarchical loss addresses this limitation. By applying part- and whole-level alignment losses to mid- and top-level representations, respectively, we achieve substantial gains over a flat loss method that naively aligns both levels only at the top layer. This result is consistent with our design philosophy: integrating localized semantics from the mid-level into a holistic representation is essential for fine-grained vision-language understanding. We further ablate the part-level alignment, relying exclusively on a whole-level loss to follow standard practices (Wu et al., 2024) (fifth row). The significant performance drop observed in this setting highlights that comprehensive scene understanding requires detailed associations between local visual and textual elements.

5. Conclusion

We introduce CAFT, a hierarchical image–text learning framework that aligns visual and textual structure across semantic scales. Our results show that cross-domain hierarchical alignment is key to unsupervised visually grounded understanding from long captions, avoiding the failure modes of global-only or local-only alignment. This hierarchical grounding improves both image-to-text and text-to-image retrieval at scale and yields more accurate zero-shot referring segmentation as a natural byproduct.

Impact Statement

This paper presents work whose goal is to advance the field of Machine Learning. There are many potential societal consequences of our work, none which we feel must be specifically highlighted here. All datasets used are publicly available, and we comply with their licenses and usage guidelines. To the best of our knowledge, the methods and findings do not pose foreseeable risks of harm, misuse, or negative societal impact.

References

Antol, S., Agrawal, A., Lu, J., Mitchell, M., Batra, D., Zitnick, C. L., and Parikh, D. Vqa: Visual question answering. In *Proceedings of the IEEE international conference on computer vision*, pp. 2425–2433, 2015.

Asokan, M., Wu, K., and Albreiki, F. Finelip: Extending clip’s reach via fine-grained alignment with longer text inputs. In *Proceedings of the Computer Vision and Pattern Recognition Conference*, pp. 14495–14504, 2025.

Bianchi, L., Carrara, F., Messina, N., Gennaro, C., and Falchi, F. The devil is in the fine-grained details: Evaluating open-vocabulary object detectors for fine-grained understanding. In *Proceedings of the IEEE/CVF Conference on Computer Vision and Pattern Recognition*, pp. 22520–22529, 2024.

Biederman, I. Recognition-by-components: a theory of human image understanding. *Psychological review*, 94(2):115, 1987.

Chalkidis, I., Dai, X., Fergadiotis, M., Malakasiotis, P., and Elliott, D. An exploration of hierarchical attention transformers for efficient long document classification. *arXiv preprint arXiv:2210.05529*, 2022.

Chen, F., Chen, X., Shi, J., Zhang, D., Chang, J., and Tian, Q. Hivlp: Hierarchical vision-language pre-training for fast image-text retrieval. *arXiv preprint arXiv:2205.12105*, 2022.

Chen, L., Li, J., Dong, X., Zhang, P., He, C., Wang, J., Zhao, F., and Lin, D. Sharegpt4v: Improving large multi-modal models with better captions. In *European Conference on Computer Vision*, pp. 370–387. Springer, 2024.

Chen, X., Xie, S., and He, K. An empirical study of training self-supervised vision transformers. In *Proceedings of the IEEE/CVF international conference on computer vision*, pp. 9640–9649, 2021.

Choi, H., Jang, Y. K., and Eom, C. Goal: Global-local object alignment learning. In *Proceedings of the Computer Vision and Pattern Recognition Conference*, pp. 4070–4079, 2025.

Dosovitskiy, A., Beyer, L., Kolesnikov, A., Weissenborn, D., Zhai, X., Unterthiner, T., Dehghani, M., Minderer, M., Heigold, G., Gelly, S., et al. An image is worth 16x16 words: Transformers for image recognition at scale. *arXiv preprint arXiv:2010.11929*, 2020.

Drozdov, A., Verga, P., Yadav, M., Iyyer, M., and McCallum, A. Unsupervised latent tree induction with deep inside-outside recursive autoencoders. In *Proceedings of the 2019 Conference of the North American Chapter of the Association for Computational Linguistics: Human Language Technologies (NAACL-HLT)*, pp. 1120–1130, 2019. URL <https://aclanthology.org/N19-1116>.

Fukushima, K. Neocognitron: A self-organizing neural network model for a mechanism of pattern recognition unaffected by shift in position. *Biological cybernetics*, 36(4):193–202, 1980.

Gao, P., Geng, S., Zhang, R., Ma, T., Fang, R., Zhang, Y., Li, H., and Qiao, Y. Clip-adapter: Better vision-language models with feature adapters. *International Journal of Computer Vision*, 132(2):581–595, 2024.

Garg, R., Burns, A., Ayan, B. K., Bitton, Y., Montgomery, C., Onoe, Y., Bunner, A., Krishna, R., Baldridge, J., and Soricut, R. Imageinwords: Unlocking hyper-detailed image descriptions. *arXiv preprint arXiv:2405.02793*, 2024.

Geng, S., Yuan, J., Tian, Y., Chen, Y., and Zhang, Y. Hiclip: Contrastive language-image pretraining with hierarchy-aware attention. *arXiv preprint arXiv:2303.02995*, 2023.

He, H., Flicke, M., Buchmann, J., Gurevych, I., and Geiger, A. Hdt: Hierarchical document transformer. *arXiv preprint arXiv:2407.08330*, 2024.

Hinton, G. Some demonstrations of the effects of structural descriptions in mental imagery. *Cognitive Science*, 3(3):231–250, 1979.

Hua, L., Su, X., Luo, Y., You, S., and Long, J. Hieclip: Hierarchical clip with explicit alignment for zero-shot anomaly detection. In *ICASSP 2025-2025 IEEE International Conference on Acoustics, Speech and Signal Processing (ICASSP)*, pp. 1–5. IEEE, 2025.

Huang, Y., Tang, J., Chen, Z., Zhang, R., Zhang, X., Chen, W., Zhao, Z., Zhao, Z., Lv, T., Hu, Z., et al. Structure-clip: Towards scene graph knowledge to enhance multi-modal structured representations. In *Proceedings of the AAAI conference on artificial intelligence*, volume 38, pp. 2417–2425, 2024.

Ilse, M., Tomczak, J., and Welling, M. Attention-based deep multiple instance learning. In *International conference on machine learning*, pp. 2127–2136. PMLR, 2018.

Jing, D., He, X., Luo, Y., Fei, N., Wei, W., Zhao, H., Lu, Z., et al. Fineclip: Self-distilled region-based clip for better fine-grained understanding. *Advances in Neural Information Processing Systems*, 37:27896–27918, 2024.

Johnson, J., Krishna, R., Stark, M., Li, L.-J., Shamma, D., Bernstein, M., and Fei-Fei, L. Image retrieval using scene graphs. In *Proceedings of the IEEE Conference on Computer Vision and Pattern Recognition (CVPR)*, pp. 3668–3678, 2015. URL https://openaccess.thecvf.com/content_cvpr_2015/html/Johnson_Image_Retrieval_Using_2015_CVPR_paper.html.

Kawamura, M., Inoue, N., Yanagi, R., Kataoka, H., and Yokota, R. Powerclip: Powerset alignment for contrastive pre-training. *arXiv preprint arXiv:2511.23170*, 2025.

Ke, T.-W., Mo, S., and Stella, X. Y. Learning hierarchical image segmentation for recognition and by recognition. In *The Twelfth International Conference on Learning Representations*, 2023.

Kim, D., Kim, N., Lan, C., and Kwak, S. Shatter and gather: Learning referring image segmentation with text supervision. In *Proceedings of the IEEE/CVF International Conference on Computer Vision*, pp. 15547–15557, 2023.

Kirillov, A., Mintun, E., Ravi, N., Mao, H., Rolland, C., Gustafson, L., Xiao, T., Whitehead, S., Berg, A. C., Lo, W.-Y., et al. Segment anything. In *Proceedings of the IEEE/CVF international conference on computer vision*, pp. 4015–4026, 2023.

Kuzovkin, I., Vicente, R., Petton, M., Lachaux, J.-P., Baciu, M., Kahane, P., Rheims, S., Vidal, J. R., and Aru, J. Activations of deep convolutional neural networks are aligned with gamma band activity of human visual cortex. *Communications biology*, 1(1):107, 2018.

Li, L. H., Zhang, P., Zhang, H., Yang, J., Li, C., Zhong, Y., Wang, L., Yuan, L., Zhang, L., Hwang, J.-N., et al. Grounded language-image pre-training. In *Proceedings of the IEEE/CVF conference on computer vision and pattern recognition*, pp. 10965–10975, 2022.

Loshchilov, I. and Hutter, F. Decoupled weight decay regularization. *arXiv preprint arXiv:1711.05101*, 2017.

Mao, J., Huang, J., Toshev, A., Camburu, O., Yuille, A. L., and Murphy, K. Generation and comprehension of unambiguous object descriptions. In *Proceedings of the IEEE conference on computer vision and pattern recognition*, pp. 11–20, 2016.

Maurer, D., Le Grand, R., and Mondloch, C. J. The many faces of configural processing. *Trends in cognitive sciences*, 6(6):255–260, 2002.

Najdenkoska, I., Derakhshani, M. M., Asano, Y. M., Van Noord, N., Worring, M., and Snoek, C. G. Tulip: Token-length upgraded clip. *arXiv preprint arXiv:2410.10034*, 2024.

Onoe, Y., Rane, S., Berger, Z., Bitton, Y., Cho, J., Garg, R., Ku, A., Parekh, Z., Pont-Tuset, J., Tanzer, G., et al. Docci: Descriptions of connected and contrasting images. In *European Conference on Computer Vision*, pp. 291–309. Springer, 2024.

Otsu, N. et al. A threshold selection method from gray-level histograms. *Automatica*, 11(285-296):23–27, 1975.

Pak, B., Woo, B., Kim, S., Kim, D.-h., and Kim, H. Textual query-driven mask transformer for domain generalized segmentation. In *European Conference on Computer Vision*, pp. 37–54. Springer, 2024.

Plummer, B. A., Wang, L., Cervantes, C. M., Caicedo, J. C., Hockenmaier, J., and Lazebnik, S. Flickr30k entities: Collecting region-to-phrase correspondences for richer image-to-sentence models. In *Proceedings of the IEEE international conference on computer vision*, pp. 2641–2649, 2015.

Radford, A., Kim, J. W., Hallacy, C., Ramesh, A., Goh, G., Agarwal, S., Sastry, G., Askell, A., Mishkin, P., Clark, J., Krueger, G., and Sutskever, I. Learning transferable visual models from natural language supervision. In Meila, M. and Zhang, T. (eds.), *Proceedings of the 38th International Conference on Machine Learning*, volume 139 of *Proceedings of Machine Learning Research*, pp. 8748–8763. PMLR, 18–24 Jul 2021. URL <https://proceedings.mlr.press/v139/radford21a.html>.

Shi, H., Mao, J., Gimpel, K., and Livescu, K. Visually grounded neural syntax acquisition. In *Proceedings of the 57th Annual Meeting of the Association for Computational Linguistics (ACL)*, pp. 1842–1854, 2019. URL <https://aclanthology.org/P19-1180>.

Song, W., Oh, S., Mo, S., Kim, J., Yun, S., Ha, J.-W., and Shin, J. Hierarchical context merging: Better long context understanding for pre-trained llms. *arXiv preprint arXiv:2404.10308*, 2024.

Sun, Q., Fang, Y., Wu, L., Wang, X., and Cao, Y. Evaclip: Improved training techniques for clip at scale. *arXiv preprint arXiv:2303.15389*, 2023.

Urbanek, J., Bordes, F., Astolfi, P., Williamson, M., Sharma, V., and Romero-Soriano, A. A picture is worth more than 77 text tokens: Evaluating clip-style models on dense captions. In *Proceedings of the IEEE/CVF Conference on Computer Vision and Pattern Recognition*, pp. 26700–26709, 2024.

Van den Bergh, M., Boix, X., Roig, G., De Capitani, B., and Van Gool, L. Seeds: Superpixels extracted via energy-driven sampling. In *European conference on computer vision*, pp. 13–26. Springer, 2012.

Vaswani, A., Shazeer, N., Parmar, N., Uszkoreit, J., Jones, L., Gomez, A. N., Kaiser, Ł., and Polosukhin, I. Attention is all you need. *Advances in neural information processing systems*, 30, 2017.

Vinyals, O., Toshev, A., Bengio, S., and Erhan, D. Show and tell: A neural image caption generator. In *Proceedings of the IEEE conference on computer vision and pattern recognition*, pp. 3156–3164, 2015.

Wang, Z., Mo, S., Yu, S. X., Behpour, S., and Ren, L. Open ad-hoc categorization with contextualized feature learning. In *Proceedings of the Computer Vision and Pattern Recognition Conference (CVPR)*, pp. 15108–15117, June 2025.

Wu, C., Wu, F., Qi, T., and Huang, Y. Hi-transformer: Hierarchical interactive transformer for efficient and effective long document modeling. *arXiv preprint arXiv:2106.01040*, 2021.

Wu, W., Zheng, K., Ma, S., Lu, F., Guo, Y., Zhang, Y., Chen, W., Guo, Q., Shen, Y., and Zha, Z.-J. Lotlip: Improving language-image pre-training for long text understanding. *Advances in Neural Information Processing Systems*, 37: 64996–65019, 2024.

Xiao, R., Kim, S., Georgescu, M.-I., Akata, Z., and Alaniz, S. Flair: Vlm with fine-grained language-informed image representations. In *Proceedings of the Computer Vision and Pattern Recognition Conference*, pp. 24884–24894, 2025.

Xie, C., Wang, B., Kong, F., Li, J., Liang, D., Zhang, G., Leng, D., and Yin, Y. Fg-clip: Fine-grained visual and textual alignment. *arXiv preprint arXiv:2505.05071*, 2025.

Xu, J., De Mello, S., Liu, S., Byeon, W., Breuel, T., Kautz, J., and Wang, X. Groupvit: Semantic segmentation emerges from text supervision. In *Proceedings of the IEEE/CVF conference on computer vision and pattern recognition*, pp. 18134–18144, 2022.

Yang, F., Sun, Q., Jin, H., and Zhou, Z. Superpixel segmentation with fully convolutional networks. In *Proceedings of the IEEE/CVF conference on computer vision and pattern recognition*, pp. 13964–13973, 2020.

Yang, J., Lu, J., Lee, S., Batra, D., and Parikh, D. Graph r-cnn for scene graph generation. In *Proceedings of the European Conference on Computer Vision (ECCV)*, pp. 670–685, 2018. URL https://openaccess.thecvf.com/content_ECCV_2018/html/Jianwei_Yang_Graph_R-CNN_for_ECCV_2018_paper.html.

Yang, Z., Yang, D., Dyer, C., He, X., Smola, A., and Hovy, E. Hierarchical attention networks for document classification. In *Proceedings of the 2016 conference of the North American chapter of the association for computational linguistics: human language technologies*, pp. 1480–1489, 2016.

Yu, L., Poirson, P., Yang, S., Berg, A. C., and Berg, T. L. Modeling context in referring expressions. In *European conference on computer vision*, pp. 69–85. Springer, 2016.

Yu, S. X., Gross, R., and Shi, J. Concurrent object recognition and segmentation by graph partitioning. In *Neural Information Processing Systems*, 2002.

Yuksekgonul, M., Bianchi, F., Kalluri, P., Jurafsky, D., and Zou, J. When and why vision-language models behave like bags-of-words, and what to do about it? *arXiv preprint arXiv:2210.01936*, 2022.

Zellers, R., Yatskar, M., Thomson, S., and Choi, Y. Neural motifs: Scene graph parsing with global context. In *Proceedings of the IEEE Conference on Computer Vision and Pattern Recognition (CVPR)*, pp. 5831–5840, 2018. URL https://openaccess.thecvf.com/content_cvpr_2018/html/Zellers_Neural_Motifs_Scene_CVPR_2018_paper.html.

Zhai, X., Mustafa, B., Kolesnikov, A., and Beyer, L. Sigmoid loss for language image pre-training. In *Proceedings of the IEEE/CVF international conference on computer vision*, pp. 11975–11986, 2023.

Zhang, B., Zhang, P., Dong, X., Zang, Y., and Wang, J. Long-clip: Unlocking the long-text capability of clip. In *European conference on computer vision*, pp. 310–325. Springer, 2024.

Zheng, K., Zhang, Y., Wu, W., Lu, F., Ma, S., Jin, X., Chen, W., and Shen, Y. Dreamlip: Language-image pre-training with long captions. In *European Conference on Computer Vision*, pp. 73–90. Springer, 2024.

Zhou, C., Loy, C. C., and Dai, B. Extract free dense labels from clip. In *European conference on computer vision*, pp. 696–712. Springer, 2022.

Appendix

In the supplemental material, we provide:

A: Additional Experimental Details

A.1: Training Datasets

A.2: Evaluation Datasets

A.3: Training Configuration

B: Additional Implementation Details

B.1: Superpixel Tokenization

B.2: Chunking

C: Additional Visual Grounding Result

D: Additional Related Works

E: Additional Visualization

E.1: Attention Map Visualization

E.2: Attention Map Visualization across Multi-Granularity

F: The Use of Large Language Model

A. Additional Experimental Details

A.1. Training Datasets

CAFT is trained on DreamLIP (Zheng et al., 2024) datasets, which consist of CC3M-recap, CC12M-recap, YFCC15M-recap and Merged-30M. In these datasets, images are re-captioned with both short and long synthetic captions generated by a diverse set of MLLMs, and we jointly use multiple types of captions during training. For the original CC3M, CC12M, and YFCC15M datasets, some images are no longer available due to their web-based nature; we therefore report the number of images actually used in our experiments for each dataset, along with the corresponding training GPU-hours, in Table 5. All experiments were conducted using 8 A100 GPUs (80GB).

Table 5. Number of images and the corresponding GPU-hours for each dataset scales.

Dataset	# Images	Training Hours	GPU Hours (Days)
CC3M-recap	2.82M	12.3	98.6 (4.1)
CC12M-recap	10.01M	42.5	340.0 (14.2)
YFCC15M-recap	14.07M	59.5	476.0 (19.8)
Merged-30M	26.90M	114.4	915.2 (38.1)

A.2. Evaluation Datasets

We present the detailed statistics of the six long-text-image retrieval datasets we use in Table 1. For DOCCI, we use only the test split for evaluation, leaving the rest untouched.

Table 6. Statistics of the long-text-image retrieval datasets.

Dataset	# Images	# Texts	# Sub-captions per Text	# Tokens per Text
DCI	7,805	7,805	10.81	172.73
DOCCI	5,000	5,000	7.12	141.52
ShareGPT4v-1k	1,000	1,000	8.15	173.24
ShareGPT4v-10k	10,000	10,000	8.24	173.66
Urban-1k	1,000	1,000	5.97	131.36
IW	612	612	10.16	239.73

A.3. Training Configuration

We follow FLAIR’s training configuration as displayed in Table 7. However, we use 2K batch size for all datasets, due to GPU RAM limit.

Table 7. Training configuration for different datasets.

Config	CC3M-recap	CC12M-recap	YFCC15M-recap	Merged-30M
Batch size		2,048		
Optimizer		AdamW (Loshchilov & Hutter, 2017)		
Learning rate		5×10^{-4}		
Weight decay	0.5	0.5	0.5	0.2
Adam β		$\beta_1, \beta_2 = (0.9, 0.98)$		
Adam ϵ	1×10^{-8}	1×10^{-8}	1×10^{-8}	1×10^{-6}
Total epochs		32		
Warm up		2,000 (steps)		
LR scheduler		cosine decay		

B. Additional Implementation Details

B.1. Superpixel Tokenization

In contrast to the square patch tokens in ViT (Dosovitskiy et al., 2020), we adopt superpixel tokens as visual units, as proposed in CAST (Ke et al., 2023). However, SEEDS (Van den Bergh et al., 2012), the superpixel segmentation algorithm utilized in CAST, struggles to capture accurate contours of thin objects and hinders hardware acceleration due to its CPU-based implementation. To address these limitations, we employ SFCN (Yang et al., 2020), a lightweight deep learning-based module for superpixel segmentation. This enables end-to-end GPU processing of the model and allows it to effectively capture thin objects, such as a broom (see Figure 8).

B.2. Chunking

In Section 3.2, we briefly introduced the idea of dividing a long caption into N sub-captions (chunks). This section provides a detailed description of the chunking strategies used in training and inference. Specifically, we adopt **random chunking** during training and **balanced chunking** during inference.

Chunking begins by splitting a long caption into L sentences:

$$S_1, S_2, \dots, S_L,$$

where L is a variable length depending on each sample.

Random chunking. During training, each chunk is formed to contain 1, 2, or 3 sentences, with the number chosen randomly. We enforce two constraints: (1) each chunk must contain at least one sentence, and (2) no chunk may contain more than three sentences. Therefore, when $L > 3N$, excess sentences are discarded. Conversely, if $L < N$, sentences are randomly resampled with replacement until all chunks are filled. We use $N = 4$; the average number of sub-captions per image for each dataset, corresponding to the mean of L , is reported in Table 6.

Balanced chunking. During inference, results may vary depending on how sentences are distributed across chunks. To ensure stable and reproducible inference, we employ balanced chunking, which divides sentences as fairly as possible. Each chunk first receives $\lfloor L/N \rfloor$ sentences, and the remaining sentences are allocated to the earlier chunks in order.

For example:

$$\begin{aligned} \text{if } L = 6, N = 4 &\Rightarrow [2, 2, 1, 1], \\ \text{if } L = 11, N = 4 &\Rightarrow [3, 3, 3, 2]. \end{aligned}$$

It is worth noting that our divide-and-conquer approach with chunking is also computationally efficient under the quadratic self-attention mechanism (Song et al., 2024). In contrast, recent CLIP variants for long-text understanding (Zhang et al., 2024; Wu et al., 2024; Asokan et al., 2025; Najdenkoska et al., 2024) process up to 248 tokens at once, leading to substantial computational cost.

C. Additional Visual Grounding Result

C.1. Fine-Grained Open-Vocabulary object Detection (FG-OVD)

We further evaluate the visual grounding capability of CAFT on the Fine-Grained Open-Vocabulary object Detection (FG-OVD) benchmark (Bianchi et al., 2024). FG-OVD assesses a model’s ability to match bounding box regions with fine-grained descriptions by asking it to distinguish the correct description from ten hard negatives. Table 8 demonstrates that CAFT exhibits superior fine-grained understanding compared to widely used Vision-Language Models, such as CLIP (Radford et al., 2021) and EVA-CLIP (Sun et al., 2023). Notably, while models trained on long captions often suffer from a lack of regional understanding (Wu et al., 2024; Bianchi et al., 2024), CAFT achieves a substantial performance margin over Long-CLIP (Zhang et al., 2024). We attribute this improvement to CAFT’s robust visual grounding capability. For a fair comparison, we report results for FG-CLIP (Xie et al., 2025) and FineCLIP (Jing et al., 2024) separately, as these methods leverage dense bounding-box annotations during training.

Table 8. FG-OVD results across difficulty levels.

Method	Hard	Medium	Easy	Trivial
<i>Trained w/o dense annotations</i>				
CLIP	12.0	23.1	22.2	58.5
EVA-CLIP	14.0	30.1	29.4	58.3
Long-CLIP	9.2	18.4	16.2	51.8
CAFT	16.8	32.8	38.6	62.5
<i>Trained w/ dense annotations</i>				
FineCLIP	26.8	49.8	50.4	71.9
FG-CLIP	46.1	66.6	68.7	83.4

D. Additional Related Works

Concurrent Segmentation and Recognition views segmentation not as an isolated task, but as an internal process that evolves alongside and supports recognition (Yu et al., 2002; Ke et al., 2023). Recent work CAST (Ke et al., 2023) adapted this paradigm to Vision Transformers (Dosovitskiy et al., 2020), demonstrating that hierarchical segmentation can be learned solely through recognition objectives, thereby revealing the intrinsic part-whole hierarchy of images. While our vision branch adopts CAST’s fine-to-coarse grouping mechanism for visual parsing, our approach diverges in two key aspects. First, we leverage language supervision as the primary recognition objective, whereas CAST relies on uni-modal discrimination (Chen et al., 2021) or fixed label supervision. Second, we explicitly encourage segment tokens to directly localize semantics via a part-level loss, in contrast to CAST, which limits supervision to the global level (i.e., [CLS] token).

Hierarchical Attention Transformers have been extensively explored in NLP domain to address the challenges of processing lengthy texts, particularly for tasks such as long document classification. Drawing inspiration from early work HAN (Yang et al., 2016), prior studies (Wu et al., 2021; Chalkidis et al., 2022; He et al., 2024) typically encode documents in a hierarchical fashion—encoding local segments individually and then aggregating them into document-level representation. However, to the best of our knowledge, such hierarchical encoding strategies remain unexplored in the domain of language-image pretraining. Inspired by the divide-and-conquer strategy with chunking (Chalkidis et al., 2022; Song et al., 2024), our hierarchical text transformer processes distinct sub-caption embeddings and aggregates them into a holistic caption representation. As this structured language modeling aligns well with the form of visual organization, it effectively prevents specific salient tokens from dominating the long caption (Wu et al., 2024).

Textual hierarchies for vision-language alignment are often inherited from linguistic structures such as syntax parses or semantic graphs. PowerCLIP (Kawamura et al., 2025) employ a syntactic parser to align image regions with a textual parse tree. Structure-CLIP (Huang et al., 2024) incorporates external semantic graph knowledge, encouraging structured image-text alignment. Although these hierarchies help compositional understanding (Yuksekgonul et al., 2022), they do not explicitly reflect how visual scenes are organized, lacking natural correspondence with the visual hierarchy. In contrast, we focus on the spatially oriented textual hierarchy inherent in long captions, where each sentence can be associated with a corresponding visual component (Zheng et al., 2024).

Hierarchical vision-language models have been relatively underexplored due to the difficulty of jointly aligning visual and textual structures. HiCLIP (Geng et al., 2023) employs a hierarchical architecture for vision and text, uncovering part-whole hierarchy for fine-grained recognition. However, HiCLIP enforces alignment only at the global level, preventing the model from learning associations among local elements. Both HiVLP (Chen et al., 2022) and HieCLIP (Hua et al., 2025) introduce multi-level alignment across different encoder depths, yet their representations remain unstructured. In contrast, our approach takes advantage of both explicit hierarchical architectures and a hierarchical alignment loss, enabling structured vision-language understanding across both local and global semantics.

E. Additional Visualization

E.1. Attention Map Visualization

We present additional attention maps from the AttnPool module for each subcaption in Figure 7. The visualizations illustrate how CAFT grounds colors, shapes, and text in images.

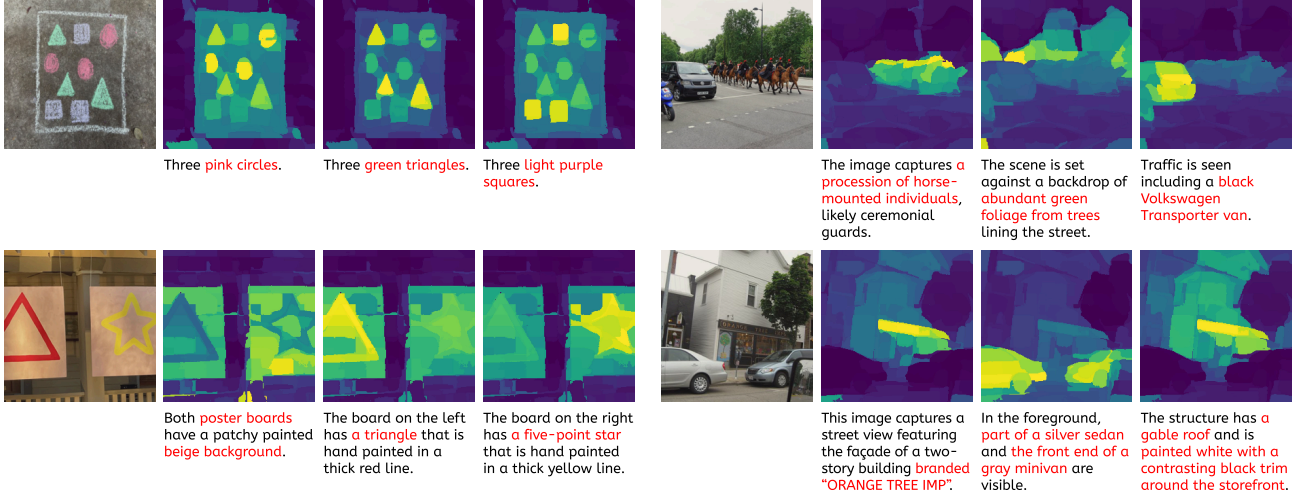


Figure 7. CAFT provides spatially grounded, compositional visual grounding. We visualize attention maps from the AttnPool module for three subcaptions in each example. The leftmost image is the input; the three heatmaps to the right show head-averaged attention with respect to each sub-caption. The scribble example shows CAFT distinguishing *pink circles* from *green triangles*. Querying with the text *ORANGE TREE IMP*, CAFT grounds it accurately. These are preliminary examples, with possible confounding factors.

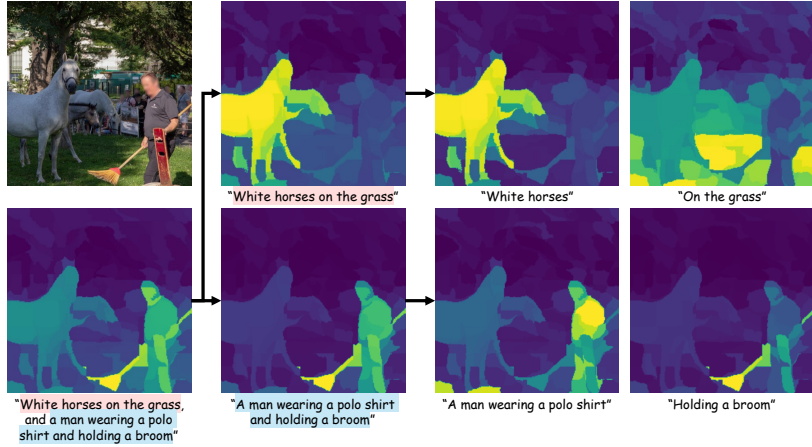


Figure 8. CAFT is capable of visual grounding across multiple levels of granularity. A single caption may describe different objects simultaneously, and can be decomposed into smaller units. To reflect this hierarchical nature of caption, we decompose the sentence-level caption into smaller phrases and visualize their corresponding grounding results. Remarkably, CAFT (1) can locate multiple objects at the same time (e.g., both *a man* and *horses* in the bottom left) and (2) precisely identify individual parts in the phrases (e.g., *holding a broom* in the bottom right).

E.2. Attention Map Visualization across Multi-Granularity

Although our training objective primarily targets the two-level spatial hierarchy that lies between the sub-caption and the full caption, our design philosophy is not restricted by the depth of hierarchy and can be naturally extended to deeper levels. We view CAFT as a first step toward even more fine-grained alignment beyond the sentence-level (i.e., aligning forest, trees, and branches). Nonetheless, we show that CAFT effectively captures multi-granular semantics within sentence-level captions,

despite not being explicitly trained for this, as shown in Figure 8. CAFT not only localizes each object individually, but can also localize multiple objects simultaneously (e.g., both the *man* and the *horses*). Moreover, when we decompose a phrase (e.g., *a man wearing a polo shirt and holding a broom*) into smaller parts (e.g., *holding a broom*), CAFT successfully grounds the corresponding part within the image.

F. The Use of Large Language Models (LLMs)

Large Language Models (LLMs) were used solely as general-purpose editing tools to refine grammar and phrasing. They did not contribute to research ideation, analysis, or substantive writing.